

<sup>16</sup>R. E. Peierls, *Phys. Rev.* **54**, 918 (1938).

<sup>17</sup>L. D. Landau and E. M. Lifschitz, *Statistical Physics* (Pergamon, London, 1959).

<sup>18</sup>For other values of the spin quantum number one cannot obtain the entropy as an explicit function of  $m$  and  $x$ . Analogous problems for any value of the spin can nevertheless be easily solved by expressing the entropy as a function of two Lagrange multipliers related to  $m$  and  $x$ . See, for instance, A. Castets, thèse de 3<sup>e</sup> cycle (Paris, 1972) (unpublished); and A. Castets and M. Nauciel-Bloch, *Solid State Commun.* (to be published).

<sup>19</sup>"Quadrupolar" ordering always occurs as a first-order transition as a consequence of Landau's theory of symmetry changes associated with phase transitions.

Indeed, the "quadrupolar" ordering corresponds to an order parameter belonging to the  $D_2$  irreducible representation of the group  $O(3)$  of all rotations around a fixed point, and the symmetrical cube of  $D_2$  contains the identical representation [cf. N. Boccara, *Ann. Phys. (N. Y.)* (to be published).] There is no such requirement for the ferromagnetic ordering, which can be (and is) found to be either first or second order.

<sup>20</sup>H. H. Chen and P. M. Levy, *Phys. Rev. Letters* **27**, 1383 (1971). In this letter a nonmagnetically ordered phase is predicted at zero temperature for isotropic and Ising-like spin-one systems with large biquadratic exchange.

## Far-Infrared Stark and Zeeman Splitting of $\text{Pr}^{3+}$ , $\text{Nd}^{3+}$ , $\text{Er}^{3+}$ , $\text{Ho}^{3+}$ , and $\text{Dy}^{3+}$ in Some Lanthanide Fluorides

Armand Hadni and Pierre Strimer  
*University of Nancy, Nancy, France*

(Received 26 October 1971)

The Zeeman effect has been studied in several rare-earth ions imbedded in lanthanide fluorides. A special cryostat has been constructed with two liquid-helium tanks. One, at 4 K, contains a superconducting coil giving magnetic fields as high as 60 kOe. The other, at 1.3 K, contains a Ge:Ga bolometer to detect far-infrared radiation. Large splittings, as high as 30  $\text{cm}^{-1}$ , have been observed with  $\text{Nd}^{3+}$ ,  $\text{Er}^{3+}$ , and  $\text{Dy}^{3+}$  where the ground state is a Kramers doublet. For  $\text{Pr}^{3+}$  and  $\text{Ho}^{3+}$ , which do not give Kramers doublets, the effect of a magnetic field is not so significant. The effect is negligible for  $\text{Pr}^{3+}$ . For  $\text{Ho}^{3+}$ , a 3- $\text{cm}^{-1}$  shift and a line broadening are observed. On the other hand, whereas the spectra of  $\text{LaF}_3:\text{Nd}^{3+}$  and  $\text{NdF}_3$  are very similar, for  $\text{PrF}_3$  a pair of ions seems to be present and gives twice as many electronic lines compared to  $\text{LaF}_3:\text{Pr}^{3+}$ . Localized modes are observed close to 73  $\text{cm}^{-1}$  for both  $\text{Er}^{3+}$  and  $\text{Dy}^{3+}$ , while an absorption band is observed at 64  $\text{cm}^{-1}$  for  $\text{Dy}^{3+}$  which seems to be slightly sensitive to the magnetic field and has still to be explained. An average spectroscopic  $g$  value for the ground-state and first-excited-state Kramers doublet has been calculated for  $\text{Nd}^{3+}$ ,  $\text{Er}^{3+}$ , and  $\text{Dy}^{3+}$ . For the ground-state Kramers doublet, these values are well within the limits of the reported  $g$  tensor based upon ESR. For the first-excited-state Kramers doublet the determinations are, respectively,  $g_2 = 1.7$ , 3.6, and 11.5 and they constitute new data.

### I. INTRODUCTION

The electric field in a crystal at a rare-earth-ion site may split the ground state to produce a series of sublevels extending from zero to a few hundred wave numbers in energy. Transitions between these sublevels may be infrared active, and a number of them have been observed at temperatures low enough to get rid of the absorption occurring from two-phonon difference modes.<sup>1</sup> Lanthanum fluoride is a good host for rare-earth ions because it can be grown in large-size crystals which are not hygroscopic.

A few studies in the far infrared have been published and a lot of low-frequency lines have been described.<sup>2-5</sup> Nevertheless, all the absorption lines are not due to electronic transitions, as we

thought in our first paper.<sup>2</sup> The spectra are certainly complicated by low-frequency infrared-active phonon modes. Fortunately, in the case of lanthanum fluoride the phonon spectrum is simple enough to make it possible to identify the pure lattice absorption unambiguously by looking at the whole series of lanthanide fluorides.

Only relatively small frequency shifts are expected from compound to compound because the increase in the rare-earth-ion mass is small from lanthanum to erbium: La = 139, Ce = 140, Pr = 141, Nd = 144, Dy = 163, Ho = 163, and Er = 168.

The increase in mass seems largely compensated by an increase of force constants due to the increase in ionic size.

The remaining absorption lines are not necessarily all due to electronic excitations. In the case

of a doped crystal, they may arise from local modes characteristic of the doping impurity, or they may reveal the whole phonon spectrum with peaks corresponding more or less accurately to maxima in the density of modes in the phonon spectrum of the host crystal. The use of a magnetic field which is efficient only on light-mass electrons is then needed to distinguish electronic transitions which can be shifted or split by the Zeeman effect from lattice excitations which are insensitive. Very high magnetic fields are necessary to modify the electronic transitions of paramagnetic ions where the magnetic-dipole moment is relatively small.

Magnetic fields as high as 50 000 to 100 000 Oe are needed, and for a long time they were at the disposal of only a few laboratories. The use of superconducting coils has now brought these facili-

ties to most physicists. However, a special cryostat has to be used with a light pipe leading the far-infrared radiation to the core of the coil where the sample is placed.

This technique is very flexible but leads to important losses of radiation and the most sensitive detector of radiation has to be used. For the past few years this detector has been a bolometer made of a germanium generally doped with gallium with a sensitivity which is two or three orders of magnitude larger than the Golay cell. This detector works at 1 K, while the superconducting coil is used at 4 K and two helium tanks are necessary for the cryostat.

Now we must not forget that all these low-lying electronic levels have energy corresponding to those of the continuum of lattice vibration frequencies. We can expect interaction of the electronic states with the nearby phonon modes. This could be detected by the breadth of the electronic lines or by a modification of some characteristic phonon lines when the magnetic field brings an electronic line close to its frequency. There are vague indications of such interactions in a few papers (Ref. 3, p. 134; Ref. 6, p. 482; Ref. 7, p. 3275).

## II. EXPERIMENTAL

The crystals are from Optovac. They are shaped into cylinders perpendicular to the  $c_3$  axis of the crystal. The cylinder is mounted in a light pipe ( $\phi = 7$  mm) coaxial with the magnetic coil (Fig. 1). The radiation entering the light pipe comes from a far-infrared grating monochromator.<sup>8</sup> The complete light pipe is separated from the monochromator by a quartz window. The other end of it holds the sample in the center of the superconducting coil and is partly filled with liquid helium. The upper vertical part of the light pipe can be removed for changing the sample. The operation takes 20 min and requires 0.1 liter of liquid helium. The small lower part under the sample cannot be removed.

The germanium bolometer is one of the best and has been described elsewhere.<sup>9</sup> It is located in a cavity communicating with the vacuum surrounding liquid-helium tank No. 1.

The radiation enters this cavity by a light pipe  $\phi = 7$  mm mechanically independent of the upper one to avoid any distortion due to a different expansion of liquid-helium tanks No. 1 and No. 2. Figure 2 gives a closer view of the germanium bolometer. The insulated copper lead to the germanium bolometer is imbedded in an indium plate in contact with the liquid-helium tank to get rid of any important heat transport from the cryostat wall to the bolometer, which has to work at the lowest possible temperature permitted by the cryostat (about 1.3 K).

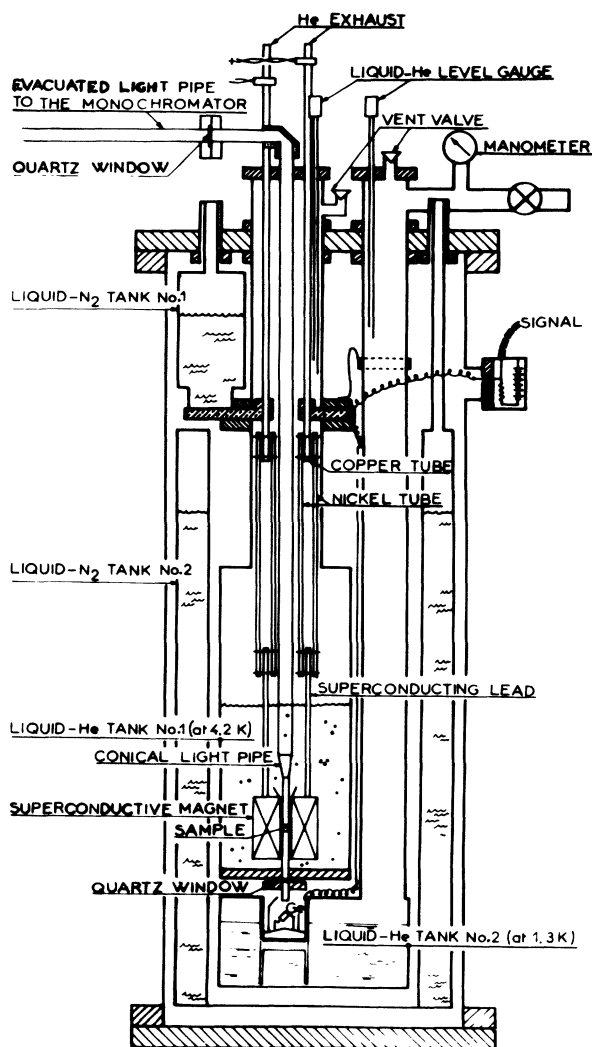


FIG. 1. Cryostat for the study of Zeeman effect in the far infrared.

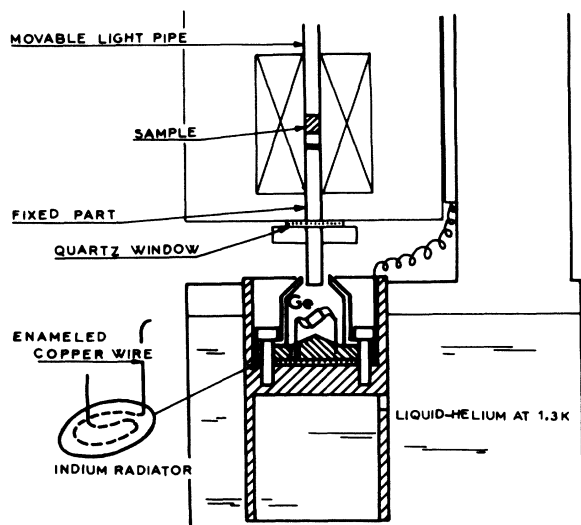


FIG. 2. Close view of the germanium bolometer.

### III. INFRARED-ACTIVE LATTICE MODES

In Fig. 3 we can see the absorption spectrum of pure lanthanum fluoride for the three possible orientations of the crystal with respect to the polarized incident beam. The  $27.5\text{-cm}^{-1}$  line is found mainly in the  $\pi$  spectrum and arises from an electric-dipole transition parallel to the  $c_3$  axis. It shifts to  $25\text{ cm}^{-1}$  when the temperature is increased from 25 to 80 K. The  $100\text{-}108\text{-}$  and  $127\text{-cm}^{-1}$  lines are found in the  $\sigma$  spectrum and ought to appear in the axial spectrum if they represent electric-dipole transitions perpendicular to the  $c_3$  axis.

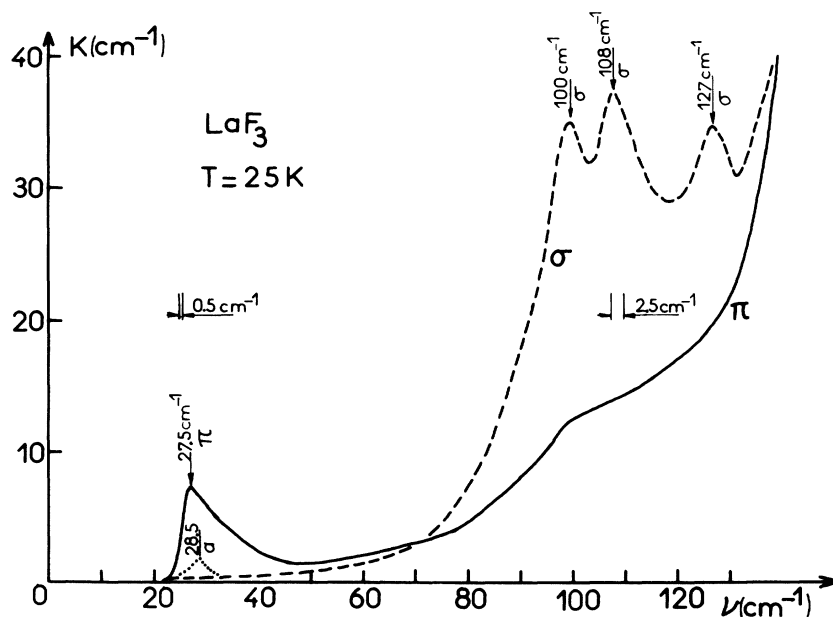


FIG. 3. Absorption coefficient of  $\text{LaF}_3$  at 25 K from 20 to  $120\text{ cm}^{-1}$  for  $\pi$  and  $\sigma$  orientations. The data are obtained from samples 1–7 mm thick.

All four lines are found in the different lanthanide fluorides and might be explained in terms of one phonon absorption at point  $\Gamma$ , though the  $27.5\text{-cm}^{-1}$  frequency gives a small absorption which disappears at room temperature,<sup>4</sup> probably because of temperature broadening. Figure 4 gives the absorption spectrum of cerium fluoride: The  $100\text{-}$  and  $108\text{-cm}^{-1}$  lines are mixed into one band but the sample is not oriented.

### IV. ELECTRONIC TRANSITIONS IN $\text{Nd}^{3+}$

#### A. Lattice Vibrations or Pure $\text{NdF}_3$

The absorption spectra of pure  $\text{NdF}_3$  in zero magnetic field have been described for axial,  $\pi$ , and  $\sigma$  polarizations.<sup>4</sup>

The lattice line at  $34\text{ cm}^{-1}$  for  $T = 18\text{ K}$  is sensitive to temperature as most lattice lines are, and is found at  $32\text{ cm}^{-1}$  for  $T = 80\text{ K}$ . It appears only in the  $\pi$  spectrum and is assigned to an electric-dipole transition parallel to the  $c_3$  axis. The  $106\text{-cm}^{-1}$  absorption band of the  $\sigma$  spectrum corresponds to the  $100\text{-}108\text{-cm}^{-1}$  lines of  $\text{LaF}_3$ , which are no longer separated in  $\text{NdF}_3$  (as in the case of  $\text{CeF}_3$ ). It is found at  $104\text{ cm}^{-1}$  in the axial spectrum (the shift is not significant because of the linewidth), and appears slightly at  $109\text{ cm}^{-1}$  in the  $\pi$  spectrum, probably because of the convergence of the beam on the sample. The band shifts to a lower frequency when the temperature is increased up to 80 K.

#### B. $45\text{-cm}^{-1}$ Band in Pure $\text{NdF}_3$

In the same way, the  $45.5\text{-}44.5\text{-}$  and  $43.5\text{-cm}^{-1}$  bands observed in spectra  $\alpha$ ,  $\pi$ , and  $\sigma$ , respectively, in pure  $\text{NdF}_3$  cannot be considered as significantly

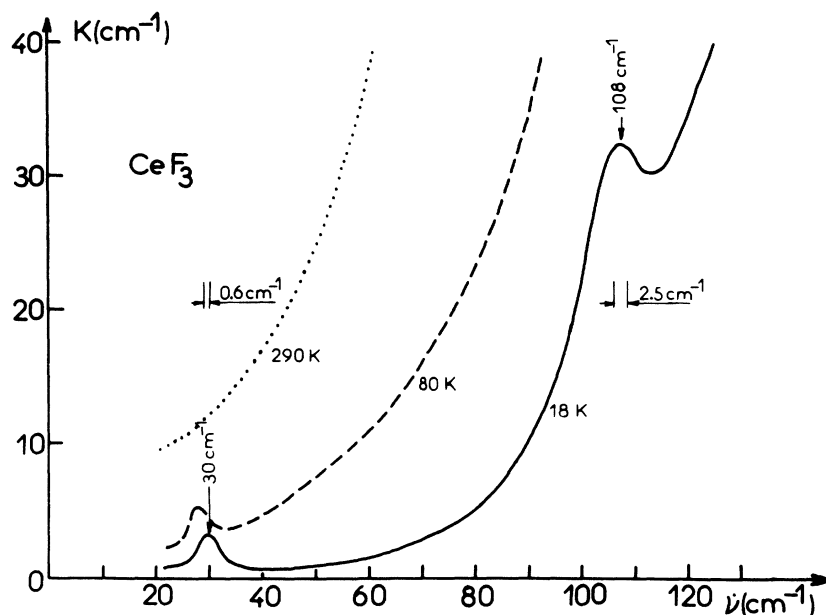


FIG. 4. Absorption coefficient of  $\text{CeF}_3$  at different temperatures (un-oriented sample).

different. The frequency does not depend upon temperature, and the intensity vanishes at room temperature. They represent one electric, non-polarized transition.<sup>3,4</sup> Figure 5 shows effectively that the line is linearly displaced by the magnetic field.

#### C. $45\text{-cm}^{-1}$ Band in $\text{LaF}_3:\text{Nd}^{3+}$

Figure 6 shows the same transition in  $\text{LaF}_3:\text{Nd}^{3+}$  in zero magnetic field (full curve). The absorption curve shows some asymmetry with a half-intensity width (about  $2.7\text{ cm}^{-1}$ ) smaller than in pure  $\text{NdF}_3$ ,

(about  $4\text{ cm}^{-1}$ ), but the frequency remains unchanged and is a good check of previous computations of the Stark splitting of the ground state  $^4I_{9/2}$  of the  $\text{Nd}^{3+}$  ions in  $\text{LaF}_3$ .<sup>10</sup>

Five Kramers doublets labeled  $Z_1-Z_5$  have been calculated.<sup>10</sup> The three lowest are represented in the center of Fig. 7. When a magnetic field is applied, the linewidth is increased up to  $7\text{ cm}^{-1}$  and its center is shifted to  $47\text{ cm}^{-1}$  for  $30\text{ kOe}$ , as in the case of pure  $\text{NdF}_3$  for the same field. However, for  $50\text{ kOe}$ , the two components are now clearly separated at  $45.5$  and  $49.5\text{ cm}^{-1}$ .

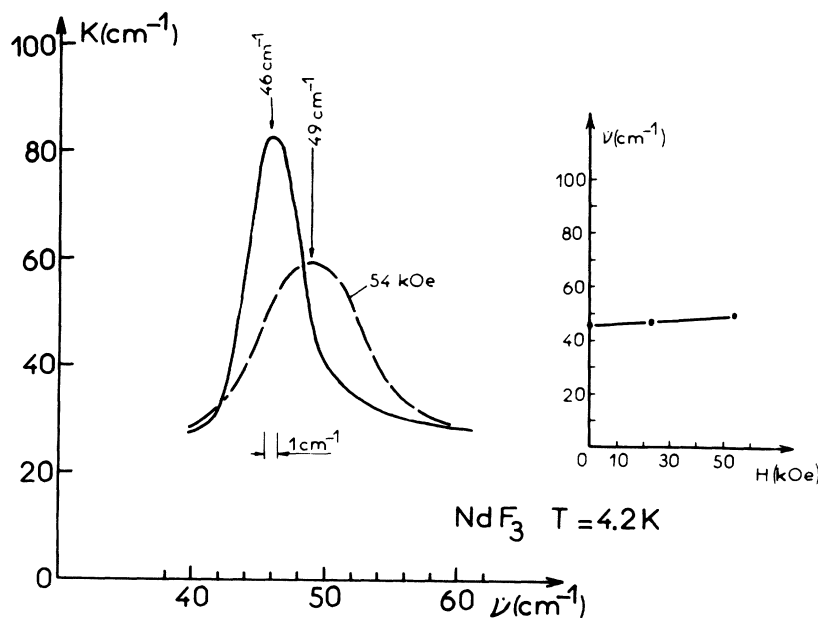


FIG. 5. Absorption coefficient of  $\text{NdF}_3$  at  $4.2\text{ K}$  around  $46\text{ cm}^{-1}$  for a  $54\text{-kOe}$  magnetic field applied perpendicular to the crystal axis. The data are obtained from a  $0.2\text{-mm}$ -thick sample.

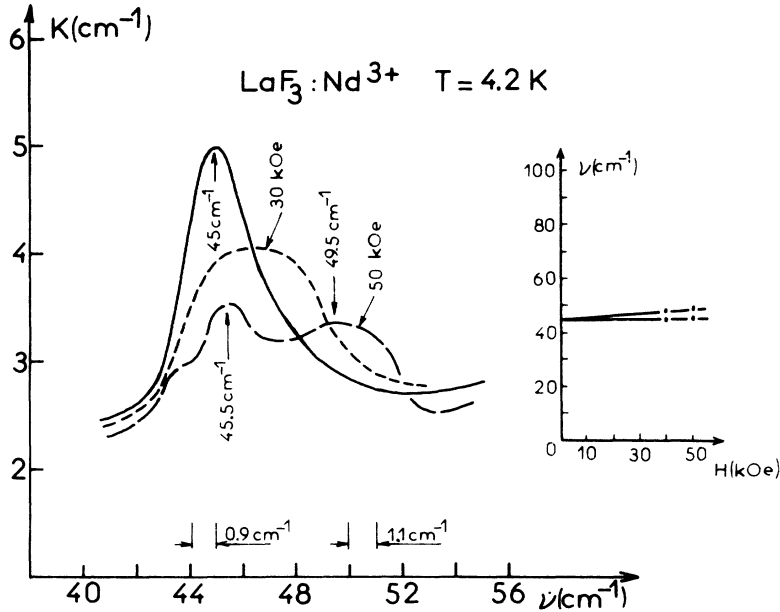


FIG. 6. Absorption coefficient of  $\text{LaF}_3:\text{Nd}^{3+}$  at 4.2 K for different magnetic fields applied perpendicular to the crystal axis. The absorption band is split into a doublet whose components are shifted linearly with the magnetic field intensity. The data are obtained from a 4-mm-thick sample.

If the ions were completely unquenched, we should use the free-ion Landé  $g$  factor given by  $g_J = \frac{3}{2} + [S(S+1) - (L+1)]/2J(J+1)$ . However, even if  $J$  is a good quantum number, and because of the crystal-field splitting of some of the  $2J+1$  different  $M_J$  states, the effective  $g$  governing the splitting may be very different from  $g_J$  and may be highly anisotropic.<sup>11</sup>

For the ground-state Kramers doublet we have

$$E_1 = -\frac{1}{2} g_1 \mu_B H,$$

$$E_2 = +\frac{1}{2} g_1 \mu_B H.$$

For the next doublet we have

$$E_3 = 45 \text{ cm}^{-1} - \frac{1}{2} g_2 \mu_B H,$$

$$E_4 = 45 \text{ cm}^{-1} + \frac{1}{2} g_2 \mu_B H.$$

$\mu_B = 0.47 \times 10^{-4} \text{ cm}^{-1} \text{ Oe}^{-1}$  is the Bohr magneton. Hence  $\mu_B H = 2.35 \text{ cm}^{-1}$  for  $H = 5 \times 10^4 \text{ Oe}$ ;  $g$  is the effective spectroscopic Zeeman factor for the ion in the crystal.<sup>12</sup> Hence we have

$$\nu_1 = E_3 - E_1 = 45 \text{ cm}^{-1} + \frac{1}{2} \mu_B H (g_1 - g_2) = 45.5 \text{ cm}^{-1},$$

$$\nu_2 = E_4 - E_1 = 45 \text{ cm}^{-1} + \frac{1}{2} \mu_B H (g_1 + g_2) = 49.5 \text{ cm}^{-1};$$

then  $g_1 = 2.13$  and  $g_2 = 1.70$ .

Now two weaker lines  $\nu_3$  and  $\nu_4$  arising from the  $E_2$  level are expected:

$$\nu_3 = 45 - 4.5 = 40.5 \text{ cm}^{-1},$$

$$\nu_4 = 45 - 0.5 = 44.5 \text{ cm}^{-1}.$$

The  $\nu_4$  frequency might explain the inflexion near  $44 \text{ cm}^{-1}$ ; the  $\nu_3$  is beyond the range of the study.

Our  $g_1$  value is very different from the free-ion

$g_J$  factor in the ground state ( $g_J = \frac{8}{11}$ ). It is not in contradiction with the electron-spin-resonance (ESR) determinations<sup>12</sup> for the ground state:  $g_2 = 3.11$ ,  $g_x = 1.356$ ,  $g_y = 1.092$ ,  $\Theta = 45^\circ$  being the angle between the  $c_3$  axis of the crystal and the  $z$  axis which is the principal direction of the  $g$  tensor corresponding to the largest principal  $g_z$  value. Our  $g$  values are close to those made previously by far-infrared techniques<sup>13</sup> where the applied magnetic field is also approximately perpendicular to the crystal axis:  $g_1 = 2.1 \pm 0.2$  and  $g_2 \approx 1.4 \pm 0.1$ . In fact, Parrish's measurements are impeded by

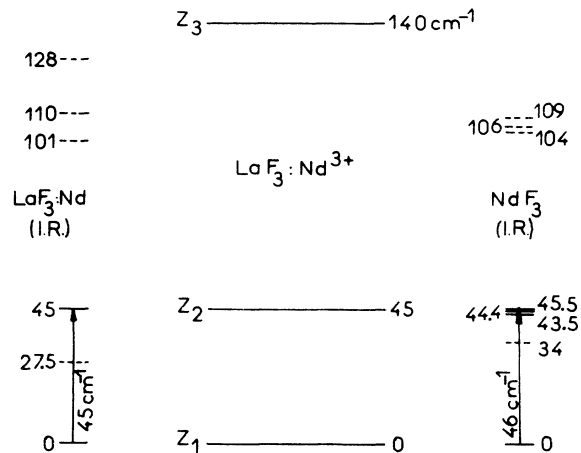


FIG. 7. Lower-energy states of  $\text{Nd}^{3+}$  in  $\text{LaF}_3$  calculated by Caspers in the center (Ref. 10) and from our measurements (left side). The right side corresponds to pure  $\text{NdF}_3$ .

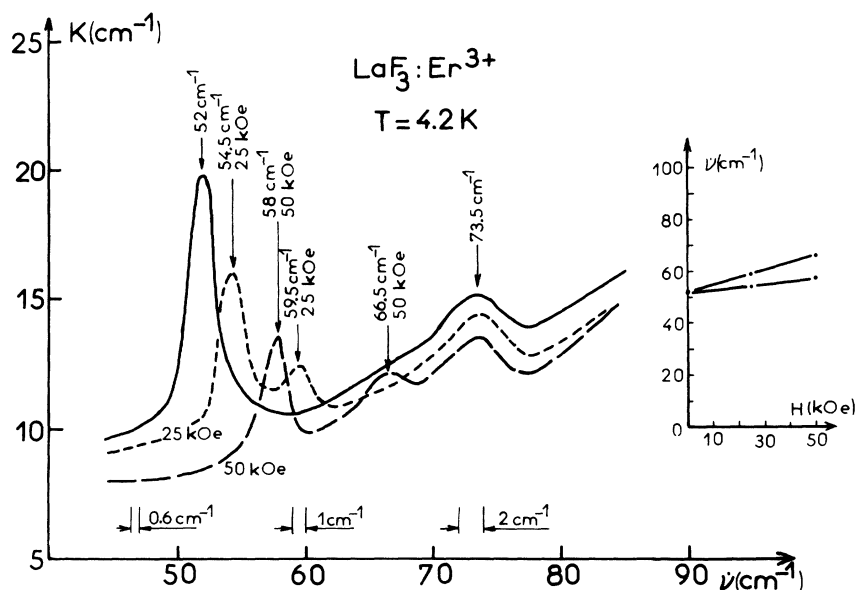


FIG. 8. Absorption coefficient of  $\text{LaF}_3:\text{Er}^{3+}$  at 4.2 K. The absorption band is split into a doublet whose components are linearly shifted by the magnetic field applied to the crystal. The crystal axis is perpendicular to the field (the data are obtained from a 1-mm-thick plate).

a weak lattice line observed at  $51\text{ cm}^{-1}$  in zero magnetic field whose intensity decreases as the magnetic field is applied. This is an argument for the authors to suggest "vibronic coupling" with the electronic transition. We did not see any evidence of this impurity lattice absorption in spite

of the very close experimental conditions (except that we used a superconducting coil instead of a Bitter magnet).

#### V. ELECTRONIC TRANSITIONS IN $\text{Er}^{3+}$ AND $\text{Dy}^{3+}$

In both cases  $J = \frac{15}{2}$  in the ground state, which

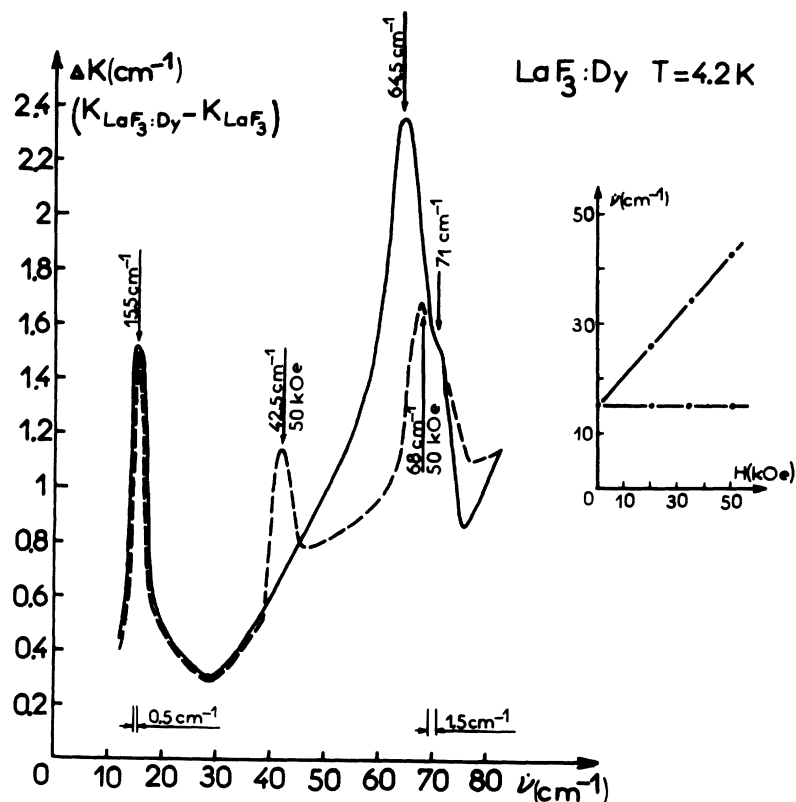


FIG. 9. Absorption coefficient  $\Delta K$  of  $\text{Dy}^{3+}$  in  $\text{LaF}_3$  at 4.2 K. The absorption band at  $15.5\text{ cm}^{-1}$  is split into a doublet. The  $15.5\text{-cm}^{-1}$  component is insensitive to the increase of the magnetic field; the other component is linearly shifted up to  $42.5\text{ cm}^{-1}$  for a 50-kOe intensity. The data are obtained from a 6-mm-thick sample.

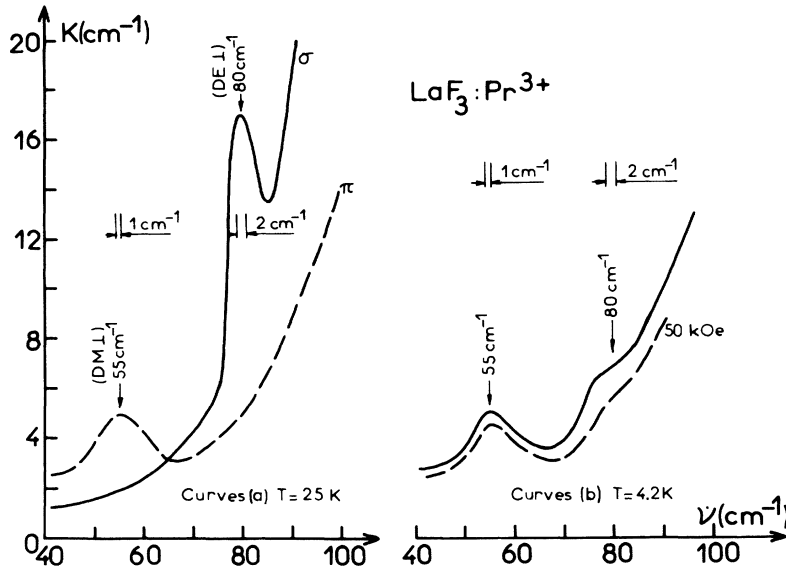


FIG. 10. Absorption coefficient of  $\text{LaF}_3:\text{Pr}^{3+}$ . The (a) curves give the  $\sigma$  and  $\pi$  spectra obtained with a sample thickness ranging from 1.5 to 7 mm. The (b) curves show the effect of a 50-kOe magnetic field applied perpendicular to the crystal axis. They are obtained with a 5.5-mm-thick sample. The radiations are nonpolarized.

thus is split into eight Kramers doublets by the  $\text{LaF}_3$  crystal field. In zero magnetic field two or three lines are found between the pure lattice absorption bands. They are located at 52 and 73.5  $\text{cm}^{-1}$  for  $\text{LaF}_3:\text{Er}^{3+}$  (Fig. 8) and at 15.5, 64.5, and 73.4  $\text{cm}^{-1}$  for  $\text{LaF}_3:\text{Dy}^{3+}$  (Fig. 9).

The action of a magnetic field splits both of the first lines at 52 and 15.5  $\text{cm}^{-1}$ , which are thus assigned to electronic transitions. It does not affect significantly the last two at 73.5 and 73.4  $\text{cm}^{-1}$ , which are thus ascribed to local modes, though the  $\text{Er}^{3+}$  ion has a larger mass (168) than the  $\text{Dy}^{3+}$  ion (163). This increase of mass is largely compensated by an increase of the force constant because of a larger ionic radius and a decrease of the lattice parameters. On the other hand, the absorption band of  $\text{Dy}^{3+}$  at 64.5  $\text{cm}^{-1}$  shows definitely a decrease of intensity when the magnetic field pushed the highest-frequency component of the electronic doublet towards its frequency. There is also a slight increase of frequency. In the case of  $\text{Er}^{3+}$ , a slight decrease of the local-mode intensity at 73.5  $\text{cm}^{-1}$  is also observed.

Now we shall look separately at each electronic transition.

#### A. Electronic Line of $\text{Er}^{3+}$ at 52 $\text{cm}^{-1}$

We shall suppose that at 4 K both lines  $\nu_1$  and  $\nu_2$  of the observed doublet are issued from the lower  $E_1$  level. Hence we have

$$\nu_1 = E_3 - E_1, \quad 58 = 52 + \left(\frac{1}{2}g_1 - \frac{1}{2}g_2\right) \mu_B H,$$

$$\nu_2 = E_4 - E_1, \quad 66.5 = 52 + \left(\frac{1}{2}g_1 + \frac{1}{2}g_2\right) \mu_B H.$$

Thus  $g_1 = 8.8$  and  $g_2 = 3.6$ . Now from ESR<sup>3</sup> for the ground state,  $g_z = 10.89$ ,  $g_x = 2.99$ , and  $g_y = 4.91$ ,

$\Theta = 45^\circ$  being the angle between the  $z$  axis and the  $c_3$  axis of the crystal.

In a different far infrared work,<sup>5</sup> where the applied magnetic field made an angle of  $45^\circ$  with respect to the optic axis of the crystal ( $90^\circ$  in our study), the Zeeman effect was said to lead to six components instead of the two that we observed. This was explained in terms of three magnetically distinguishable erbium substitutional sites in  $\text{LaF}_3$ . There is definitely not any absorption line at frequencies lower than 55  $\text{cm}^{-1}$  in our 50-kOe spectrum, while they described three Zeeman-component frequencies ranging from 50 to 55  $\text{cm}^{-1}$ . They

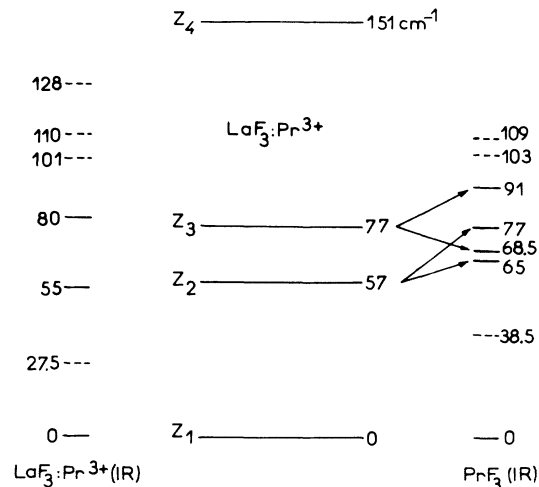


FIG. 11. Lower energy levels of  $\text{LaF}_3:\text{Pr}^{3+}$  as they have been observed (left side) and as they have been calculated by Caspers (center). The right side shows the energy levels that we have observed for pure  $\text{PrF}_3$ .

were led to  $g$  values ranging from 7.5 to 1.5.

#### B. Electronic Lines in $Dy^{3+}$ at $15.5\text{ cm}^{-1}$

Let us assume the same scheme for  $Dy^{3+}$  as for  $Er^{3+}$ . We have

$$\nu_1 = 15.5 = 15.5 + \frac{1}{2}(g_1 - g_2) \mu_B H,$$

$$\nu_2 = 42.5 = 15.5 + \frac{1}{2}(g_1 + g_2) \mu_B H.$$

Hence  $g_1 = g_2 = 11.5$ . Now from ESR<sup>12</sup> for the ground state,  $g_x = 13.8$ ,  $g_y = 7$ ,  $g_z = 1.5$ , and  $\Theta = 9^\circ$ .

#### VI. ELECTRONIC TRANSITIONS IN $Pr^{3+}$

Figure 10 (on the left side) gives the  $\sigma$  and  $\pi$  spectra of  $LaF_3:Pr^{3+}$  showing two lines at  $55\text{ cm}^{-1}$  ( $\pi$ ) and  $80\text{ cm}^{-1}$  ( $\sigma$ ) which could pretty well fit the  $Z_1 - Z_2$  and  $Z_1 - Z_3$  transitions indicated in the center of Fig. 11, where the energies of the levels have been taken from spectroscopic measurement in the visible region.<sup>4</sup> Nevertheless, we see in Fig. 10 (on the right side) that the action of a 50-kOe magnetic field is negligible. We must recall that there are no Kramers doublets in the case of  $Pr^{3+}$  where  $J = 4$ , with a ground state  $^3H_4$  which is split completely into nine sublevels in the low-symmetry ( $C_{2v}$ ) crystalline field of the  $LaF_3$  host at the site of the ion. The Zeeman effect is a second-order effect<sup>13</sup> and appears to be negligible in this experiment.

In the case of pure  $PrF_3$  four lines have been described<sup>2</sup> between the lattice absorption bands at 38 and  $91\text{ cm}^{-1}$ , as can be seen in Fig. 11 (right side). Here again no shift is observed under the action of a magnetic field (Fig. 12), except a narrowing of the  $65\text{-cm}^{-1}$  absorption band. Nevertheless, the 69-

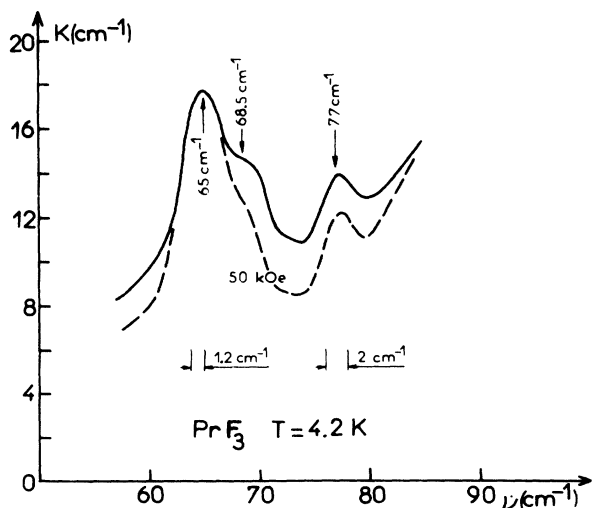


FIG. 12. Absorption coefficient of pure  $PrF_3$  at 4.2 K with and without a magnetic field applied perpendicular to the crystal axis. The data are obtained from a 1.3-mm-thick sample.

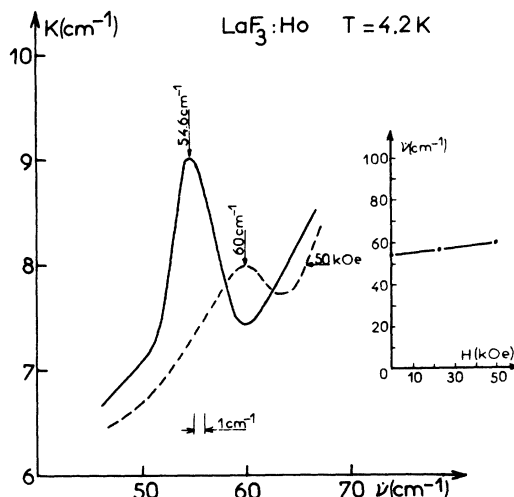


FIG. 13. Absorption coefficient of  $LaF_3:Ho^{3+}$ . The absorption band at  $54.6\text{ cm}^{-1}$  is shifted to  $60\text{ cm}^{-1}$  when a 50-kOe magnetic field is applied perpendicular to the  $c_3$  axis. The linewidth is increased from 4 to about  $10\text{ cm}^{-1}$ . The data are obtained from a 3-mm-thick sample.

and  $77\text{-cm}^{-1}$  lines occur predominantly in the  $\pi$  spectrum as the  $55\text{-cm}^{-1}$  line found in  $LaF_3:Pr^{3+}$ , while the 91- and  $68\text{-cm}^{-1}$  lines are mostly in the  $\sigma$  spectrum as the  $80\text{-cm}^{-1}$  line of  $LaF_3:Pr^{3+}$ . Hence the possibility of an explanation in terms of a coupling between two praseodymium ions, splitting the  $80\text{-cm}^{-1}$   $\sigma$  line into the 91- and  $68\text{-cm}^{-1}$  components ( $D_{E\perp}$ ) and splitting the  $55\text{-cm}^{-1}$   $\pi$  line into the 65- and  $77\text{-cm}^{-1}$  components ( $D_{M\perp}$ ).

Let us recall that all four components are found in the axial spectrum and have been classified as perpendicular electric-dipole ( $D_{E\perp}$ ) and perpendicular magnetic-dipole ( $D_{M\perp}$ ) transitions, as is pointed out above. The  $55\text{-cm}^{-1}$  absorption band of  $LaF_3:Pr^{3+}$  should be  $D_{M\perp}$ , and the  $80\text{-cm}^{-1}$  band should be  $D_{E\perp}$ . The same characters are observed for the band of pure  $PrCl_3$  at 31 and  $100\text{ cm}^{-1}$ , and no splitting is observed which could be an indication of coupling between pairs of ions in that case.

#### VII. ELECTRONIC TRANSITION IN $Ho^{3+}$

In  $Ho^{3+}$  there are ten  $4f$  electrons and the ground state  $^5I_8$  will be split into seventeen Stark levels by the crystal field in  $LaF_3$ ; only one far-infrared absorption band is observed in  $LaF_3:Ho^{3+}$  besides the lattice absorption. It is located at  $54.6\text{ cm}^{-1}$ , with a  $4\text{-cm}^{-1}$  width (Fig. 13). While  $LaF_3:Pr^{3+}$  was not significantly sensitive to a magnetic field, here we observe a shift towards higher frequencies, a decrease of peak intensity, and a broadening of the band. We can assume that we observe either the unresolved splitting of a first excited Stark level or the shift of a single first excited Stark level.

In the second assumption the broadening should



occur from different possible sites of the  $\text{Ho}^{3+}$  ion which might have different  $g$  values, hence from several components which should not be separated.

#### VIII. CONCLUSION

The study of a series of lanthanum fluorides either pure or doped has enabled us to describe four lattice vibrations which are located at  $27.5 \text{ cm}^{-1}$  ( $\pi$  component) and  $100\text{--}108$  and  $127 \text{ cm}^{-1}$  ( $\sigma$  component) for  $\text{LaF}_3$  at 25 K. Specific electronic transitions have been demonstrated in  $\text{Nd}^{3+}$ ,  $\text{Er}^{3+}$ ,  $\text{Dy}^{3+}$ , and  $\text{Ho}^{3+}$  by the effect of a magnetic field with dramatic shifts as high as  $30 \text{ cm}^{-1}$  for 50 kOe in the case of  $\text{Dy}^{3+}$ . However, the light-pipe geometry precluded any precise Zeeman study with polarized radiation. Moreover, there are six ions in the unit cell with

identical but differently oriented  $g$  tensors. They are derived from one another by  $120^\circ$  rotation about the crystal axis and reflection in the plane perpendicular to it.<sup>12</sup> Each of the six lanthanide sites will have a slightly different Zeeman splitting. Consequently, only an average spectroscopic  $g$  value for the six lanthanide sites could be determined in our experiments where the magnetic field is located in a direction perpendicular to the  $c_3$  axis of the crystal. For the ground Kramers doublet these  $g_1$  values are 2.13, 8.8, and 11.5 for  $\text{Nd}^{3+}$ ,  $\text{Er}^{3+}$ , and  $\text{Dy}^{3+}$ , respectively, which is well within the limits of the reported  $g$  tensor based upon the electron spin resonance.<sup>12-15</sup> For the first-excited-state Kramers doublet the  $g_2$  values are 1.7, 3.6, and 11.5 and could not be determined from ESR.

<sup>1</sup>A. Hadni, Phys. Rev. **136**, A758 (1964).

<sup>2</sup>A. Hadni and P. Strimer, Compt. Rend. **265**, 811 (1967).

<sup>3</sup>J. F. Parrish, R. P. Lowndes, and C. H. Perry, Phys. Letters **29A**, 133 (1969).

<sup>4</sup>A. Hadni, P. Strimer, and F. Vermillard, Compt. Rend. **269**, 1113 (1969).

<sup>5</sup>J. F. Parrish, C. H. Perry, and P. R. Lowndes, Phys. Letters **31A**, 263 (1970).

<sup>6</sup>J. C. Hill and R. G. Wheeler, Phys. Rev. **152**, 482 (1966).

<sup>7</sup>D. Bloor and J. A. Campbell, J. Chem. Phys. **54**, 3268 (1971).

<sup>8</sup>A. Hadni, *Essentials of Modern Physics Applied to the Infrared* (Pergamon, Oxford, 1967), p. 642.

<sup>9</sup>A. Hadni, P. Strimer, R. Thomas, M. Dugue, F. J. Gremillet, and N. Moulin, Phys. Status Solidi **5**, 707 (1971).

<sup>10</sup>H. H. Caspers, H. E. Rast, and R. A. Buchanan, J. Chem. Phys. **42**, 3214 (1965).

<sup>11</sup>M. Tinkham, Phys. Rev. **124**, 311 (1961).

<sup>12</sup>J. M. Baker and R. S. Rubins, Proc. Phys. Soc. (London) **78**, 1353 (1961).

<sup>13</sup>A. J. Sievers and M. Tinkham, Phys. Rev. **124**, 321 (1961).

<sup>14</sup>H. H. Caspers, H. E. Rast, and R. A. Buchanan, J. Chem. Phys. **43**, 2124 (1965).

<sup>15</sup>J. H. Van Vleck and M. H. Bebb, Proc. Amsterdam Acad. **32**, 17 (1934).